Theory of Linear Optical Absorption in B_{12} Clusters: Role of the geometry

Sridhar Sahu and Alok Shukla
*Department of Physics, Indian Institute of Technology, Bombay, Powai, Mumbai 400076, INDIA**

Boron clusters have been widely studied theoretically for their geometrical properties and electronic structure using a variety of methodologies. An important cluster of boron is the B_{12} cluster whose two main isomers have distinct geometries, namely, icosahedral (I_h) and quasi planar (C_{3v}). In this paper we investigate the linear optical absorption spectrum of these two B_{12} structures with the aim of examining the role of geometry on the optical properties of clusters. The optical absorption calculations are performed using both the semi-empirical and the *ab initio* approaches. The semi-empirical approach uses a wave function methodology employing the INDO model Hamiltonian, coupled with large-scale configuration interaction (CI) calculations, to account for the electron-correlation effects. The *ab initio* calculations are performed within a time-dependent-density-functional-theory (TDDFT) methodology. The results for the two approaches are in very good qualitative agreement with each other. Quantitatively speaking, results agree with each other in the lower energy region, while in the higher energy region, features predicted by the TDDFT approach are red-shifted as compared to the INDO-CI results. Both the approaches predict that the optical absorption begins at much lower energies in the icosahedral cluster as compared to the planar one, a fact which can be utilized in experiments to distinguish between the two geometries. At higher energies, both the isomers exhibit plasmon-like excitations.

PACS numbers: 36.40.Vz, 31.10.+z,31.15.bu,31.15.vq

I. INTRODUCTION

In the recent years, the study of the boron clusters has attracted considerable attention due to their potential applications as hydrogen storage devices,[1,2] hard semiconducting solids and various other properties.[3,4] Extensive theoretical studies of one-, two-, and three-dimensional boron clusters of different sizes have been carried out by various researchers.[5,6,7,8,9,10,11,12,13,14,15] Of these, icosahedral B_{12} cluster[3] has generated a lot of interest in recent years possibly because of its high symmetry and its occurrence as the fundamental structural unit in crystalline boron, and various boron-rich solids.[16,17]In an early work Bambakidis and Wagner[5] computed the structural and cohesive properties of icosahedral B_{12} using the SCF-Xα-SW approach, and estimated its HOMO-LUMO gap. Kawai and Ware[6] employed Car-Parinello *ab initio* molecular dynamics approach to analyze the structural instabilities of cage-like B_{12}. Kato and Yamashita[7] performed *ab initio* Hartree-Fock calculations to optimize the geometries of various neutral and cationic boron clusters, and obtained a triplet ground state with a trigonal bipyramid structure for the B_{12} cluster. Boustani,[8,9] using both *ab initio* density-functional theory (DFT),[8] and wave function based quantum-chemical[9] approaches, presented detailed studies of various boron clusters, including several structural isomers of B_{12}. Using a semiempirical approach, Fujimori and Kimura[10] explored the nature of bonding in icosahedral clusters of group III atoms, including cage-like B_{12}. Hayami,[11] using an *ab initio* DFT based approach studied the encapsulating properties of the icosahedral B_{12}. Zhai *et al.*,[12] in a recent joint theoretical and experimental study investigated some small boron clusters, including B_{12}, and argued that these clusters prefer planar aromatic structures. In a first-principles study, He *et al.*,[13] explored the ionicities of boron-boron bond in icosahedral B_{12} caused by symmetry breaking. Atis *et al.*,[14] based upon an *ab initio* DFT methodology, presented a theoretical study of several neutral boron clusters, along with an analysis of relative stability of various isomers, including B_{12} isomers. Prasad and Jemmis[15] in a first principles study examined the structure of several large boron clusters and concluded that the ones constructed from the B_{12} icosahedron as the basic unit are more stable as compared to the fullerene-like structures.

In spite of several studies of structural properties of boron clusters, very few studies of their dielectric response properties exist. For example, Reis *et al.*,[18,19] computed the static linear and nonlinear optical susceptibilities of rhombic B_4 clusters using a first-principles methodology. In an earlier work, by means of *ab initio* correlated calculations, we had computed the static dipole polarizabilities of ladder-like boron clusters.[20] Although optical absorption spectra of icosahedral clusters of atoms such as Al and Pb have recently been computed,[21] to the best of our knowledge, no such calculations for the linear or non-linear optical response of B_{12} clusters (quasi-planar or icosahedral) have been performed. Given the fact that B_{12} clusters were recently discovered experimentally,[12] it is of considerable interest to compute their optical properties. Theoretical calculations of optical absorption spectra, coupled with the experimental measurements, can be used to identify clusters of various shapes and sizes, and to distinguish between various isomers. With this aim in mind, we present a theoretical study of the frequency-dependent linear optical response of B_{12} icosahedral cluster, as well as its quasi-planar isomer which was recently discovered experimentally by Zhai *et al.*[12] Such comparative stud-

ies are important because they also help us in understanding the role of geometry in the optical response of clusters. Our calculations have been performed using both a semiempirical INDO[22] model based approach within the configuration-interaction (CI) framework, as well as an *ab initio* time-dependent density functional theory (TDDFT) based methodology.[23,24] Linear optical absorption spectra computed using the two approaches are in full qualitative agreement with each other. Regarding quantitative aspects, agreement in the lower energy region is very good, while the TDDFT results are redshifted as compared to the INDO-CI results in the high energy region. The predictions of our calculations can be tested in future optical absorption experiments on these clusters.

Remainder of the paper is organized as follows. In the next section we present the theoretical aspects of our approach, to be followed by the presentation and discussion of our results in section III. Finally, in section IV we present the conclusions

II. THEORETICAL BACKGROUND

For the present study, we adopted a wave-function based electron-correlated methodology employing the semi-empirical intermediate-neglect of differential overlap (INDO) model developed by Pople and coworkers.[22,25] The INDO model, like its predecessor complete neglect of differential overlap (CNDO) model,[26] employs an effective valence-electron Hamiltonian which uses Slater-type-orbital (STO) as basis functions, and several of its one- and two-electron integrals are approximated using a semi-empirical parameterization scheme. The main difference between the INDO and the CNDO models is that, in the INDO model one-center Coulomb repulsion integrals include more nonzero terms as compared to the CNDO model, leading generally to a better description of the excited state energies. For a detailed discussion of the theory behind these approaches, and essential differences therein, we refer the reader to the book by Pople and Beveridge.[25]

We adopted a semi-empirical approach, as against a fully *ab intio* one, because, with twelve atoms, an *ab initio* correlated calculation with even modest-sized basis sets becomes intractable. On the other hand, the INDO method, with its smaller basis set (four basis functions per atom), allows one to treat electron-correlation effects at a much higher level than what is feasible using an *ab initio* approach. Our calculations are initiated at the Hartree-Fock (HF) level, within the INDO model, using a computer program developed recently by us.[33] The INDO-HF molecular orbitals (MOs), are used to transform the Hamiltonian from the original atomic-orbital (AO) to the MO representation, which is subsequently used in the post-HF correlated calculations.

There are several variants of the INDO approach in vogue which differ from each other in terms of the semi-empirical parameters used. In this work we have used the original INDO parameterization proposed by Pople and coworkers.[22] For the calculations of spectroscopic properties such as the excitation energies, CNDO/S[27] and the INDO/S[28,29,30] approaches have been used so frequently that it is virtually impossible to cite all of them. INDO/S method was parameterized by Zerner and coworkers[28,29,30] to reproduce spectra of small aromatic molecules with the use of low-order CI approaches, such as the singles-CI (SCI) method. However, when Adachi and Nakamura benchmarked the performance of the INDO/S method for the case of organic dyes, they found that the excitation energies obtained were significantly blue-shifted as compared to the experimental results.[31] This led the authors to conclude that while the INDO/S method performs well for the ultraviolet region of the spectrum possibly because it was parameterized for small aromatic molecules, its performance is not all that good in the visible region of the spectrum.[31] Therefore, we decided to use the original INDO parameters,[22] coupled with a high-level correlation scheme (see below) so that the influence of parameters is neutralized to a certain extent. Indeed, recently El-Shahawy *et al.*[32] also used this original INDO approach[22] to calculate the excitation energies of the paracetamol molecule successfully. However, to further benchmark our INDO-CI approach, as well as to approach the problem from a complementary perspective, we have also performed calculations of the optical absorption spectra of the two isomers using the *ab initio* TDDFT approach.[23,24] This, we believe, has helped us tremendously in critically analyzing our INDO-CI results.

The correlated calculations, beyond the INDO-HF, are performed using the multi-reference singles-doubles configuration-interaction (MRSDCI) approach as implemented in the computer program MELD.[34] MRSDCI approach is a well-established quantum-chemical approach in which one considers singly- and doubly-excited configurations from a number of reference configurations, leading to a good treatment of electron correlations both for the ground and the excited states, in the same calculation. Using the ground- and excited-state wave functions obtained from the MRSDCI calculations, electric dipole matrix elements are computed and subsequently utilized to compute the linear absorption spectrum assuming a Lorentzian line shape. By analyzing the wave functions of the excited states contributing to the peaks of the computed spectrum obtained from a given calculation, bigger MRSDCI calculations are performed by including a larger number of reference states. The choice of the reference states to be included in a given calculation is based upon the magnitude of their contribution to the CI wave function of the excited state (or states) contributing to a peak in the spectrum. This procedure is repeated until the computed spectrum converges within an acceptable tolerance, and all the configurations contributing significantly to various excited states are included in the list of the reference states. In the past, we have used such an

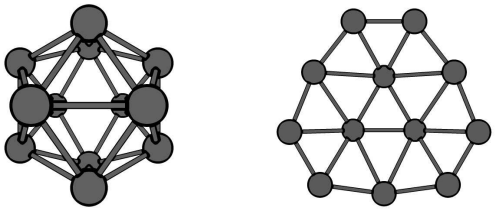

(a) (b)

Figure 1: Structures of: (a) icosahedral (I_h) and, (b) quasi-planar (C_{3v}) clusters of B_{12} considered in these calculations.

iterative MRSDCI approach on a number of conjugated polymers to perform large-scale correlated calculations of their linear and nonlinear optical properties.[35]

III. CALCULATIONS AND RESULTS

A. Geometries

In Figs. 1a and 1b we depict the structures of the icosahedral (I_h) and quasi-planar (C_{3v}) isomers of B_{12}, respectively. The ground state optimized geometries of both the isomers of B_{12} were obtained at the INDO-HF level. For the icosahedron we obtained the edge length to be 1.702 Å which is virtually identical to that obtained by Hayami for the same structure.[11] In order to further ensure that our geometry was reasonable, using the Gaussian03[39] program we also performed geometry optimization for both the isomers within the DFT approach, employing the B3LYP functional, and a 6-31g(d) basis set. This calculation also yielded the edge-length of 1.70 Å for the I_h structure, in perfect agreement with our INDO-HF results, and those of Hayami.[11] For the quasi-planar structure of C_{3v} symmetry, we used the geometry optimized by Boustani with the bond lengths 1.60 Å, 1.64 Å, and 1.65 Å.[9] Our own B3LYP/6-31g(d) optimization for this system yields corresponding bond lengths to be 1.63 Å, 1.66 Å, and 1.68 Å, again in good agreement with the results of Boustani.[9] However, our results both at the INDO-HF and the INDO-CI level predict cage structure to be more stable as compared to the planar one, which is exactly opposite to the result obtained by Boustani.[9] In a recent experimental study Zhai *et al.*[12] discovered the quasi-planar B_{12} isomer, without ruling out the possibility that the larger planar boron clusters will eventually fragment into B_{12} icosahedra. The purpose of our work, in any case, is not to examine the relative stability of the two isomers, but to investigate their linear optical response.

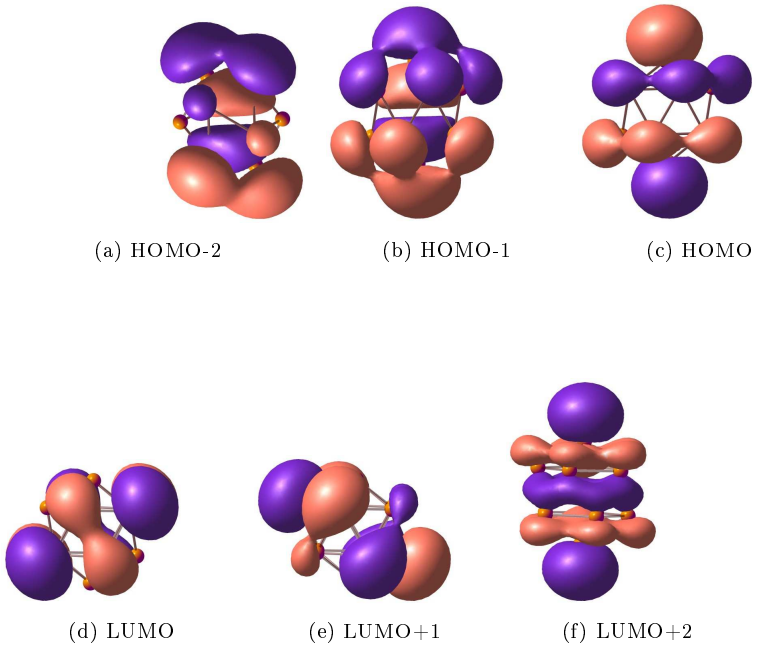

(a) HOMO-2 (b) HOMO-1 (c) HOMO

(d) LUMO (e) LUMO+1 (f) LUMO+2

Figure 2: (Color online) Molecular orbitals (iso plots) of icosahedral B_{12} obtained from INDO-HF calculations.

B. Molecular Orbitals

Next we present the plots of the molecular orbitals (MOs) of both the icosahedral and quasi-planar B_{12} obtained from the INDO-HF calculations, in Figs. 2 and 3, respectively. Molecular orbitals presented here are close to the Fermi level, and corresponding orbitals obtained from the first principles DFT/B3LYP calculations are presented in Figs. 7 and 8 of the Appendix. Orbital energies of some of the INDO-HF orbitals are presented in Table I. Upon comparing the MOs obtained from INDO-HF calculations to those of DFT/B3LYP calculations presented in these figures, we find perfect agreement as to the qualitative nature of the orbitals. Regarding the quantitative aspects, the DFT/B3LYP MOs are expectedly more diffuse as compared to the INDO-HF ones, because they employ an extended basis set.

Because of the inversion symmetry of icosahedral B_{12}, its MOs are either symmetric (*gerade*) with respect to the inversion operation, or antisymmetric (*ungerade*) with respect to it. From Fig. 2 it is obvious that all the MOs from HOMO-2 to LUMO+1 have *ungerade* symmetry while LUMO+2 has *gerade* symmetry. This implies that HOMO→LUMO transition is dipole disallowed, and, therefore, the closest orbital to which HOMO electrons can be optically excited is LUMO+2. Moreover, orbitals LUMO and LUMO+1 are degenerate (*cf.* Table I) because of the symmetry. The charge density distribu-

Orbitals	Orbital Energy (eV)	
	Quasi-planar (C_{3v})	Icosahedral (I_h)
HOMO-5	-16.227	-14.749
HOMO-4	-15.227	-14.719
HOMO-3	-15.219	-8.770
HOMO-2	-15.219	-8.731
HOMO-1	-10.490	-8.349
HOMO	-10.490	-3.684
LUMO	0.287	2.475
LUMO+1	0.287	2.475
LUMO+2	0.841	3.476
LUMO+3	3.833	3.593
LUMO+4	5.297	3.633
LUMO+5	5.297	4.028

Table I: INDO canonical Hartree-Fock orbital energies of some of the orbitals close to the Fermi level for both the quasi-planar and the cage-like B_{12}clusters.

tion of HOMO (*cf.* Fig. 2c) is concentrated near the two pentagons, and vertex atoms on top/bottom of it, with negligible charge in between the two pentagons. Thus, compared to HOMO, it can be argued that the charge distribution of LUMO+2 (*cf.* Fig. 2f) can be obtained by transferring some charge from pentagon and top/bottom atoms, to the region between the two pentagons.

Quasi-planar (C_{3v}) isomer of B_{12} lacks inversion symmetry so that its molecular orbitals cannot be classified as *gerade* or *ungerade*, a fact which is obvious from the MO plots presented in Fig. 3. As a result of this, the HOMO→LUMO transition is dipole allowed. However, symmetry C_{3v} of the system manifests itself in form of orbital degeneracies, with HOMO being degenerate with HOMO-1, and LUMO with LUMO+1 (*cf.* Table I). The charge distribution in HOMO-1 and HOMO is fairly delocalized with most regions of the cluster covered, while for LUMO and LUMO+1 it is mainly concentrated on the edge atoms, with central triangle having negligible charge.

C. Optical Absorption Spectra

In this section we present the results of our INDO-CI and first-principles TDDFT calculations of the linear optical absorption spectra of the two isomers.

Even with a valence electron approximation the number of orbitals involved in the INDO-CI calculation is rather large (18 occupied and 30 virtual orbitals) and can lead to very large CI expansions. We solve this problem by freezing occupied orbitals far away from the Fermi level. This orbital freezing is carried out in a systematic manner, and the convergence of the results with respect to the total number of frozen orbitals (N_{freez}) is carefully examined in Appendix B.

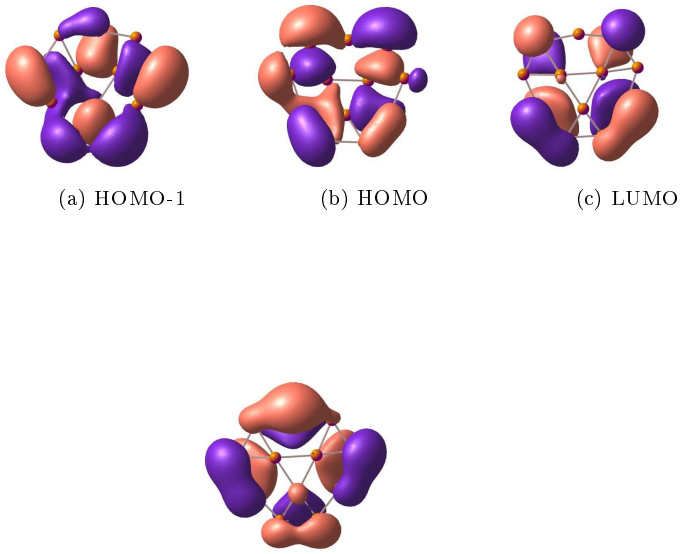

(a) HOMO-1 (b) HOMO (c) LUMO

(d) LUMO+1

Figure 3: (Color online) Molecular orbitals (iso plots) of quasi-planar B12 obtained from the INDO-HF calculations.

For the cage, we only utilized the inversion symmetry (symmetry group C_s), so that the orbitals and the many-electron states can be classified into A_g (*gerade*) and A_u (*ungerade*) irreducible representations (irreps). The ground state belongs to the A_g irrep, while the one-photon excited states belong to the A_u irrep. Our final MRSDCI results for the icosahedral structure were obtained by freezing twelve occupied orbitals ($N_{freez} = 12$) both for the A_g and A_u symmetry manifolds. For the quasi-planar isomer, point-group symmetry was not used, and thus, the ground, and the excited states, were computed in the same MRSDCI calculation. The total number of CI configurations used in the MRSDCI calculation is about one million in case of cage structure, and over half a million in case of quasi-planer structure. From the sizes of these CI matrices it is obvious that these calculations are fairly large-scale, and that the electron-correlation effects are properly accounted for. The detailed analysis of the convergence of our results with respect to the number of the reference states (N_{ref}) used in the MRSDCI calculations, and, therefore, the size of the CI matrix, has been provided in Appendix. B

The linear absorption spectrum was computed using the sum-over-states approach, with the total number of excited states ranging anywhere from fifty to hundred. Obtaining that many excited states from large MRSDCI calculations was a computationally expensive task, and

Table II: Excitation energies, E, and many-particle wave functions of the excited states corresponding to some of the peaks in the INDO-MRSDCI linear absorption spectrum of icosahedral B_{12} (*cf.* Fig. 4a), along with the squares of their dipole coupling ($\mu^2 = \sum_i |\langle f|d_i|G\rangle|^2$) to the ground state. $|f\rangle$ denotes the excited state in question, $|G\rangle$, the ground state, and d_i is the i-th Cartesian component of the electric dipole operator. In the wave function, the bracketed numbers are the CI coefficients of a given electronic configuration. Symbols H/L denote HOMO/LUMO orbitals. Same information about rest of the peaks can be found in table IV of the Appendix C.

Peak	E (eV)	μ^2(a.u.)	Wave Function
I	0.8745	0.0391	$\|H \rightarrow L+5\rangle(0.5818)$
			$\|H \rightarrow L+1; H \rightarrow L+2\rangle(0.4295)$
			$\|H \rightarrow L; H \rightarrow L+3\rangle(0.3355)$
			$\|H \rightarrow L; H \rightarrow L+6\rangle(0.3036)$
II	1.3642	0.2215	$\|H \rightarrow L+3\rangle(0.5821)$
			$\|H \rightarrow L+5\rangle(0.3354)$
			$\|H \rightarrow L+1; H \rightarrow L+2\rangle(0.3330)$
			$\|H \rightarrow L; H \rightarrow L+3\rangle(0.3152)$
III	3.4416	0.1486	$\|H \rightarrow L+2\rangle(0.4449)$
			$\|H \rightarrow L+1; H \rightarrow L+3\rangle(0.3560)$
			$\|H \rightarrow L; H \rightarrow L+2\rangle(0.3496)$
			$\|H \rightarrow L+4\rangle(0.3346)$
VI	6.7030	0.2619	$\|H \rightarrow L+10\rangle(0.3260)$
			$\|H \rightarrow L+1; H \rightarrow L+8\rangle(0.2449)$
			$\|H-1 \rightarrow L+2\rangle(0.2380)$
	6.7366	0.1417	$\|H \rightarrow L+9\rangle(0.3778)$
			$\|H \rightarrow L; H \rightarrow L+10\rangle(0.2895)$
	6.7564	0.3198	$\|H \rightarrow L+10\rangle(0.5598)$
			$\|H \rightarrow L; H \rightarrow L+9\rangle(0.3254)$
VIII	7.7822	0.3373	$\|H-3 \rightarrow L+6\rangle(0.3285)$
			$\|H-3 \rightarrow L+1; H \rightarrow L+4\rangle(0.2601)$
			$\|H-3 \rightarrow L; H \rightarrow L+3\rangle(0.2586)$
	7.9592	0.1889	$\|H \rightarrow L+1; H-3 \rightarrow L+6\rangle(0.2851)$
			$\|H-2 \rightarrow L+2\rangle(0.2586)$
			$\|H-1 \rightarrow L; H \rightarrow L+1;$ $H \rightarrow L+4\rangle(0.2514)$
	8.0153	0.1343	$\|H-3 \rightarrow L; H \rightarrow L+6\rangle(0.2837)$
			$\|H-3 \rightarrow L+5\rangle(0.2096)$

took several days for some calculations on our computer cluster, running dual-CPU quad-core processors. Our INDO-MRSDCI linear absorption spectra of the cage and planar isomers are presented in Figs. 4 and 5, respectively. With the purpose of benchmarking our INDO-CI approach, and also to study these systems from a complementary perspective, we performed *ab initio* TDDFT calculations of the absorption spectrum of both the isomers. For the purpose we used the same geometry as

Table III: This table contains information pertinent to some of the peaks of INDO-MRSDCI optical absorption spectrum of the quasi-planar B_{12} as shown in Fig. 5a. The symbols have the same meaning as in the caption of table II. Same information about rest of the peaks can be found in table V of the Appendix C.

Peak	E(eV)	μ^2(a.u.)	Wave function
I	4.6844	0.0960	$\|H-1 \rightarrow L+1\rangle(0.7525)$
			$\|H \rightarrow L\rangle(0.5714)$
			$\|H-1 \rightarrow L; H \rightarrow L+1\rangle(0.1271)$
II	8.4488	0.3599	$\|H \rightarrow L+3\rangle(0.8665)$
			$\|H-3 \rightarrow L\rangle(0.1808)$
			$\|H \rightarrow L+4\rangle(0.1673)$
			$\|H-1 \rightarrow L+5\rangle(0.1361)$
			$\|H-4 \rightarrow L+1\rangle(0.1278)$
			$\|H \rightarrow L+1; H \rightarrow L+2\rangle(0.3330)$
III	8.9674	0.1690	$\|H-1 \rightarrow L+2\rangle(0.4386)$
			$\|H-1 \rightarrow L+5\rangle(0.4044)$
			$\|H \rightarrow L+4\rangle(0.3889)$
			$\|H-3 \rightarrow L+2\rangle(0.3457)$
			$\|H-2 \rightarrow L+1\rangle(0.2625)$
			$\|H-4 \rightarrow L+1\rangle(0.2528)$
			$\|H \rightarrow L+6\rangle(0.2008)$
IV	9.4482	0.0505	$\|H-3 \rightarrow L+1\rangle(0.6229)$
			$\|H-2 \rightarrow L\rangle(0.4281)$
			$\|H-1 \rightarrow L; H \rightarrow L+1\rangle(0.2539)$
			$\|H-1 \rightarrow L+4\rangle(0.2457)$
			$\|H-2 \rightarrow L+2\rangle(0.2268)$

those for the INDO calculations, and used the GAUSSIAN 03 package,[39] coupled with the 6-31g(d) basis set, and B3LYP gradient hybrid correlation functional. These TDDFT absorption spectra are also presented in Figs. 4 and 5.

Upon comparing the INDO-MRSDCI results with the *ab initio* TDDFT ones, we conclude that the spectra computed by the two approaches are in very good qualitative agreement with each other, with both sets of spectra exhibiting weak absorption at lower energies, and very intense absorptions at high energies. Next, we make a quantitative comparison between the spectra computed by the INDO-MRSDCI and TDDFT approaches, for both the isomers.

For the icosahedral cluster (*cf.* Fig. 4) the two spectra exhibit the onset of optical absorption close to 0.9 eV in form of low intensity peaks, (b) next set of low intensity peaks starts a little below 4 eV in both the spectra; in the INDO spectrum these peaks continue beyond 4 eV, while in the TDDFT spectrum they are all below 4 eV, and (c) high energy feature of both the spectra are dominated by very high-intensity peaks which occur above 6 eV in the INDO spectrum and between 4 eV and 5 eV in the TDDFT spectrum. Thus, we have very good agreement

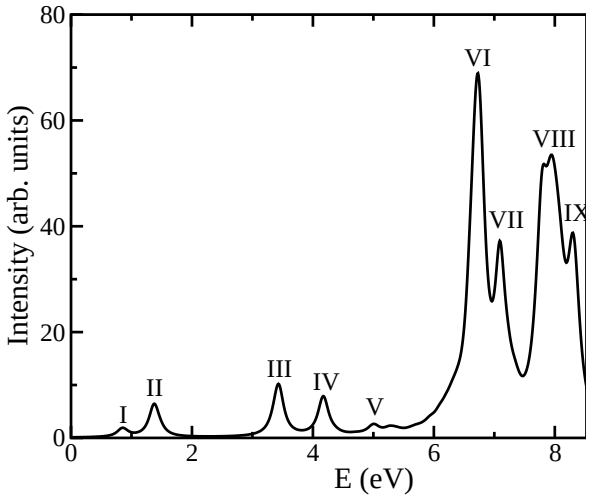

(a) INDO-MRSDCI spectrum

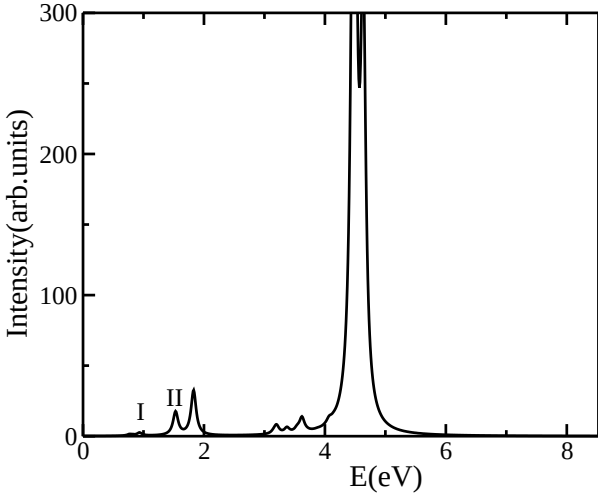

(b) TDDFT spectrum

Figure 4: Linear optical absorption spectrum of icosahedral B_{12} computed using: (a) the

between the spectra for the first set of peaks around 0.9 eV and the second set of peaks at energies close to 4 eV. For high-energy features we have a disagreement in that the INDO theory predicts these features at energies higher than 6 eV while the *ab initio* TDDFT predicts them between 4 and 5 eV.

Upon comparing the INDO-MRSDCI and TDDFT spectra for the quasi-planar isomer (*cf.* Fig. 5), a similar picture emerges. In the INDO-MRSDCI spectrum the first, relatively weak, peak occurs at around 4.7 eV followed by a set of strong peaks beyond 8 eV, with the intermediate region (4.7 eV — 8.4 eV) exhibiting almost negligible absorption. The TDDFT spectrum is slightly different with the first weak peak close to 4.04 eV, followed by a slightly stronger peak at 5.27 eV. Really intense peaks in the TDDFT spectrum occur in the energy range between 5.9 eV and 7 eV. Therefore, the quantitative comparison between the INDO-MRSDCI and TDDFT spectra for the quasi-planar isomer is quite similar to that of the icosahedral isomer. Agreement is reasonable for the lower energy peaks, but for the higher peaks, TDDFT spectrum is significantly redshifted as compared to the INDO-MRSDCI spectrum. Qualitatively, however, both sets of spectra are in very good agreement with each other.

Next we present a detailed comparative analysis of our INDO-MRSDCI results for the cage and the quasi-planar structures. To facilitate this comparison visually, we also present a combined plot of the two spectra in Fig. 6. A cursory look at Fig. 6 reveals that lower energy regions of the absorption spectra consist of relatively lower intensity peaks while the higher energy spectra in both the isomers exhibit intense absorption. A comparison of the the spectra of the two isomers reveals that: (a) the absorption spectrum of the icosahedral isomer is significantly red-shifted as compared to the planar one, and (b) the peak intensities in both the spectra are of the same order of magnitude. The main distinguishing feature of the absorption spectra of the two isomers, as depicted by our calculations, is that in the icosahedral B_{12} the optical absorption (*cf.* Fig. 4) begins at rather low energies with the first peak (peak I) located at 0.86 eV, with two more peaks (peaks II and III) located below 4 eV, while in the quasi-planar isomer (Fig. 5) the first absorption absorption feature (peak I) is located significantly higher at 4.73 eV. This INDO-MRSDCI result is also confirmed in the TDDFT calculations, which also predict the absorption to commence at much lower energies in the icosahedral isomer, as compared to the quasi-planar one (*cf.* Figs. 4b and 5b). This prediction of our calculations can be tested in future experiments on boron clusters, and if confirmed, can be used for distinguishing the icosahedral clusters from the quasi-planar ones in optical absorption experiments.

As far as the higher energy features are concerned, in the icosahedral cluster (Fig. 4), a series of high intensity features (peaks V, VI, VII, and VIII) start around 6.7 eV and continue past 8 eV. In the planar isomer (Fig. 5) on the other hand the higher energy absorptions (peaks

II through VII) start beyond 8 eV and continue to much higher energies beyond 12 eV.

The many-particle wave functions of the excited states corresponding to some of the peaks in the spectra, along with the squares of their transition dipoles, are presented in Tables II and III. The same information about the rest of the peaks can be examined in tables IV and V of Appendix C. One distinguishing feature of the optical absorption in cage, compared to that in the quasi-planar isomer is that HOMO (H) to LUMO (L) transition is dipole forbidden in the cage because, as discussed above, H and L orbitals have the same inversion symmetry of u, and among the unoccupied orbitals, $L+2$ is the lowest-lying with the opposite symmetry of g, thereby making $H \rightarrow L+2$ as the lowest allowed single-particle optical transition for the cage. For the quasi-planar B_{12} on the other hand, the single-particle transition $H \rightarrow L$ is optically allowed because the system does not have inversion symmetry.

Before further discussions of our results it is useful to remember that in the crystalline form boron is a semiconductor, with an indirect band gap close to 1.53 eV for β-rhombohedral boron,[36] whose crystal structure is also based on B_{12} icosahedron. Semiconductors exhibit single-particle inter-band optical absorption at lower energies, and collective plasmon absorption at high energies. Therefore, it is of interest to understand the optical absorption spectra of B_{12} clusters based on these pictures and to ascertain whether absorption exhibits single-particle behavior or the collective one. Indeed for the case of metallic clusters such as those of alkali metals the issue, whether the optical excitations are similar to those in a molecule, or they are related to the plasmons in the bulk, has been extensively examined.[37] In metal cluster physics plasmon excitations are identified by appearance of continuous absorption pattern. Moreover, Koutecký and coworkers[38] have devised a scheme according to which if the many particle wave function of a given excited state is dominated by one singly-excited configuration it is classified as a normal inter-band absorption.

On the other hand if the excited state wave function is a linear combination of several configurations with similar weights, it is called a collective (plasmon like) excitation.[38] Close examination of the many-particle wave functions of both the isomers presented in Tables II, III, IV, and V reveals that none of the excited states participating in the optical absorption of B_{12} clusters are dominated by single configurations. All these excited states have prominent multi-reference character, and are linear combinations of several singly- and doubly-excited configurations with significant coefficients. For example, peaks I of both the isomers are a mixture of singly and doubly excited configurations, as are all the other peaks. This, as per the criterion outlined in the work of Koutecký and coworkers,[38] suggests plasmon like behavior. Moreover, the absorption spectrum appears to be fairly continuous starting with low-energy and low-intensity absorptions, followed by high-energy high-intensity absorptions before tapering off.

IV. CONCLUSIONS AND FUTURE DIRECTIONS

In conclusion, we have presented a theoretical study of linear optical absorption in two B_{12} isomers, namely icosahedral and quasi-planar clusters. The wave-function-based calculations were performed using the semi-empirical INDO model,[22] and electron correlation effects were taken into account by means of large-scale MRSDCI computations. To obtain an alternative perspective on the optical absorption, TDDFT method based *ab initio* calculations of the spectrum were also performed. A comparison of the INDO-MRSDCI and TDDFT calculations revealed that the two methods lead to spectra which are qualitatively very similar. On the quantitative front, the high-energy features of spectra were found to be red-shifted in the TDDFT approach as compared to the INDO-MRSDCI approach. Which of these results is closer to reality can only be decided by the experiments, which, we hope will be performed in the future. Another aspect of these spectra is that the optical absorption in the icosahedral clusters begins at much lower energies as compared to the planar one, a fact which can be used in the optical detection of these clusters. The high-intensity absorption in the cluster takes place at higher energies, which our calculations suggest, are plasmonic in nature. Results of these calculations, which to the best of our knowledge have not been performed earlier, can be tested in the future experiments. It will also be interesting to investigate the nature of triplet excited states in boron based clusters along with their nonlinear optical properties. Calculations along those directions are in progress in our group, and results will be presented in future publications.

* Electronic address: sridhar@phy.iitb.ac.in, shukla@phy.iitb.ac.in

[1] T. Ozturk, A. Demirbas, Energy Sources, Part A **29**, 1415 (2007).
[2] M. L. McKee, Z. Wang and P. v R. Schleyer, J. Am. Chem. Soc. **122**, 4781 (2000).
[3] E.L Mutterties, 'The Chemistry of Boron and its Compounds', Wiely, New York, 1968.
[4] W. L. Lipscomb, 'Boron Hydrides', W. A. Benjamin, New York, 1963.
[5] G. Bambakidis and R. P. Wagner, J. Phys.Chem. Solids **42**,1023 (1981).

[6] R. Kawai and J. H. Weare, J. Chem. Phys. **95**, 1151 (1991).
[7] H. Kato and K. Yamashita, Chem. Phys. Lett. **190**, 361(1992).
[8] I. Boustani, Chem. Phys. Lett. **240**, 135 (1995).
[9] I. Boustani, Phys. Rev. B **55**, 16426 (1997).
[10] M. Fujimori and K. Kimura, J. Sol. St. Chem. **133**, 310 (1997).
[11] W. Hayami, Phys.Rev. **B** 60,1523 (1999).
[12] H. J. Zhai, B. Kiran, J. LI, and L. S. Wang, Nature Mat. **2**, 827 (2003).
[13] J. He, E. Wu, H. Wang, R. Liu, and Y. Tian, Phys. Rev. Letts. **94**, 015504 (2005).
[14] M. Atis, C. Özdoğan, and Z. B. Güvenç, Int. J. Quant. Chem. **107**, 729 (2007).
[15] D. L. V. K. Prasad and E. D. Jemmis, Phys. Rev. Lett. **100**, 165504 (2008).
[16] C. L. Perkins, M. Trenary and T. Tanaka, Phys. Rev. Lett. **77**, 4772 (1996).
[17] H. Hubert, B. Devouard, L. A. J. Garvie, M. O'Keeffe, P. R. Buseck, W. T. Petuskey and P. F. McMillan, Nature **391**, 376 (1998).
[18] H. Reis and M. G. Papadopoulos, J. Comp. Chem. **20**, 679 (1999).
[19] H. Reis, M. G. Papadopoulos, and I. Boustani, Int. J. Quant. Chem. **78**, 131 (2000).
[20] A. Abdurahman, A. Shukla, and G. Seifert, Phys. Rev. B **66**, 155423 (2002).
[21] R. Xie, G. W. Bryant, J. Zhao, T. Kar and V. H. Smith Jr., Phys. Rev. B **71**, 125422 (2005).
[22] J. A. Pople, D. L. Beveridge and P. A. Dobosh, J. Chem. Phys. **47**, 2026 (1967).
[23] A. Zangwill and P. Soven, Phys. Rev. A **21**, 1561 (1980).
[24] E. Runge and E. Gross, Phys. Rev. Lett. **52**, 997 (1984).
[25] For a review, see, *e.g.*, J. A. Pople and D. L. Beveridge , Approximate Molecular Orbital Theory, McGraw-Hill Publications, 1970.
[26] J.A. Pople, D.P. Santry, and G.A. Segal, J. Chem. Phys. **43**, S 129 (1965); J.A. Pople and G.A. Segal, J. Chem. Phys. **43**,S136 (1965); J.A. Pople and G.A. Segal, J. Chem. Phys. **44**, 3289 (1966).
[27] J. D. Bene and H. H. Jaffé, J. Chem. Phys. 48, 1807 (1968).
[28] J. E. Ridley and M. C. Zerner, Theor. Chim. Acta **32**, 111 (1973).
[29] A. D. Bacon and M. C. Zerner, Theoret. Chim. Acta **53,** 21 (1979).
[30] M. C. Zerner, G. H. Loew, R. F. Kirchner, and U. T. Mueller-Westerhoff, J. Am. Chem. Soc. **102**,589 (1980).
[31] M. Adachi and S. Nakamura, Dyes and Pigments **17**, 287 (1991).
[32] A. S. El-Shahawy, S. M. Ahmed, and N. Kh. Sayed, Spectrochimica Acta Part A **66**, 143 (2007).
[33] S. Sahu and A. Shukla, Comp. Phys. Comm. **180**, 724 (2009).
[34] We used modules sortin, cistar, rtsim and tmom of MELD, a molecular electronic structure program from University of Indiana with contributions from E. R. Davidson, L. McMurchie, S. Elbert, and S. Langhoff.
[35] See, *e.g.*, P. Sony and A. Shukla, J. Chem. Phys. **131**, 014302 (2009); P. Sony and A. Shukla, Phys. Rev. B **75**, 155208 (2007); P. Sony and A. Shukla, Phys. Rev. B **71**, 165204 (2005); A. Shukla, Phys. Rev. B **65**, 125204 (2002).
[36] H. Werheit, A. Hausen, and H. Binnerbruck, Phys. Stat. Solidi **42**, 733 (2006).
[37] W. A. de Heer, Rev. Mod. Phys. **65**, 611 (1993).
[38] J. Blanc, V. Bonačić-Koutecký, M. Broyer, J. Chevaleyre, Ph. Dugourd, J. Koutecký, C. Scheuch, J. P. Wolf, and L. Wöste, J. Chem. Phys. **96**, 1793 (1992).
[39] Gaussian 03, Revision C.02, M. J. Frisch, G. W. Trucks, H. B. Schlegel, G. E. Scuseria, M. A. Robb, J. R. Cheeseman, J. A. Montgomery, Jr., T. Vreven, K. N. Kudin, J. C. Burant, J. M. Millam, S. S. Iyengar, J. Tomasi, V. Barone, B. Mennucci, M. Cossi, G. Scalmani, N. Rega, G. A. Petersson, H. Nakatsuji, M. Hada, M. Ehara, K. Toyota, R. Fukuda, J. Hasegawa, M. Ishida, T. Nakajima, Y. Honda, O. Kitao, H. Nakai, M. Klene, X. Li, J. E. Knox, H. P. Hratchian, J. B. Cross, V. Bakken, C. Adamo, J. Jaramillo, R. Gomperts, R. E. Stratmann, O. Yazyev, A. J. Austin, R. Cammi, C. Pomelli, J. W. Ochterski, P. Y. Ayala, K. Morokuma, G. A. Voth, P. Salvador, J. J. Dannenberg, V. G. Zakrzewski, S. Dapprich, A. D. Daniels, M. C. Strain, O. Farkas, D. K. Malick, A. D. Rabuck, K. Raghavachari, J. B. Foresman, J. V. Ortiz, Q. Cui, A. G. Baboul, S. Clifford, J. Cioslowski, B. B. Stefanov, G. Liu, A. Liashenko, P. Piskorz, I. Komaromi, R. L. Martin, D. J. Fox, T. Keith, M. A. Al-Laham, C. Y. Peng, A. Nanayakkara, M. Challacombe, P. M. W. Gill, B. Johnson, W. Chen, M. W. Wong, C. Gonzalez, and J. A. Pople, Gaussian, Inc., Wallingford CT, 2004.

Appendix A: MOLEULAR ORBITALS OF B_{12} ISOMERS OBTAINED FROM *AB INITIO* CALCULATIONS

In this section we present some of the molecular orbitals of icosahedral and quasi-planar isomers of B_{12}, obtained from the first-principles DFT calculations employing B3LYP functional, and the 6-31g(d) gaussian basis set. The calculations were performed using the Gaussian03 program,[39] and the orbitals presented are the ones close to the Fermi level. In Fig. 7 orbitals of icosahedral isomer are plotted, while in Fig. 8 those of the quasi-planar isomer are presented. These orbitals agree quite well with the corresponding orbitals obtained from the INDO-HF calculations, presented in Figs. 2 and 3 of the main text.

Appendix B: CONVERGENCE ISSUES

In this section we discuss the convergence of our MRSDCI calculations with respect to: (a) the number of frozen orbitals N_{freez}, and (b) the number of reference configurations N_{ref}, with respect to which the singly- and doubly-excited configurations spanning the CI space are generated. For a given value of N_{freez}, successively larger MRSDCI calculations (*i.e.* with the increasing values of N_{ref}) were performed, until no significant changes in the results were observed both with respect to, decreasing N_{freez}, and increasing N_{ref}. In Fig. 9 we present the results of the best (largest N_{ref}) MRSDCI calculations on the icosahedral B_{12} with $N_{freez} = 16$, 14, and 12, and $N_{ref} = 83$, 92, and 84, respectively. In these calculations the sizes of the MRSDCI matrices (N_{total}) ranged

from 20935 for $N_{freez} = 16$ to 940945 for $N_{freez} = 12$. From the figure it is obvious that there are no significant qualitative or quantitative changes in the absorption spectrum as N_{freez} is decreased from fourteen to twelve. Similarly, Fig. 10 demonstrates the convergence of the absorption spectrum with respect to increasing N_{ref} (and hence N_{tot}), with values $N_{ref} = 1$, 60, 79, and 84. Thus, we can conclude that our results for the cage B_{12} are well converged both with respect to N_{freez} as well as N_{ref}.

Similar checks of convergence were also performed for the quasi-planar isomer of B_{12}, figures corresponding to which are not presented here for the reasons of brevity.

Appendix C: EXCITED STATE WAVE FUNCTIONS, ENERGIES, AND TRANSITION MOMENTS

In the following two tables we present the excitation energies, the many-particle wave functions, and the transition dipole moments with respect to the ground state, of the excited states corresponding to those peaks in the INDO-MRSDCI linear absorption spectra of the two isomers of B_{12}, which were not included in the tables II and III of Sec. III.

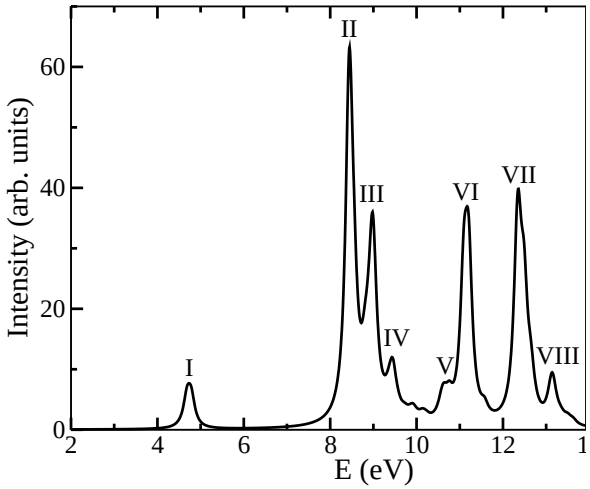

(a) INDO-MRSDCI spectrum

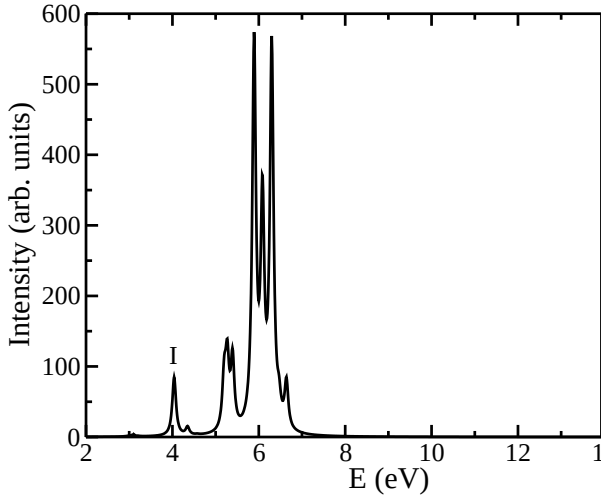

(b) TDDFT spectrum

Figure 5: Linear optical absorption spectrum of quasi-planner B_{12} computed using: (a) the INDO-MRSDCI method, with $N_{freez} = 12$ and $N_{ref} = 31$, and (b) TDDFT method using 6-31g(d) basis set and B3LYP functional. A line width of 0.1 eV was used to compute the spectra in both the cases.

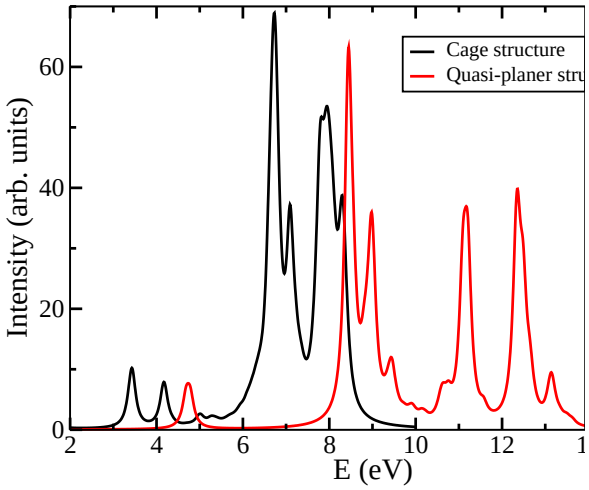

Figure 6: (color online) Comparison of the linear optical spectra of icosahedral (black) and quasi-planar (red) structures of B_{12}cluster.

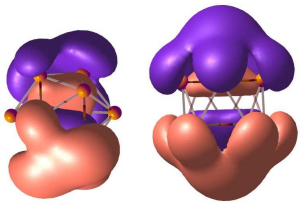

(a) HOMO-2 (b) HOMO-1

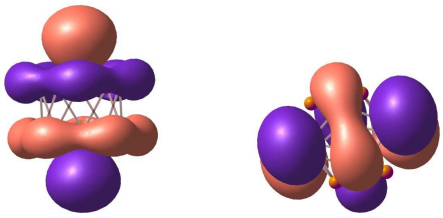

(c) HOMO (d) LUMO

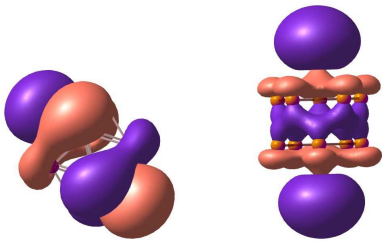

(e) LUMO+1 (f) LUMO+2

Figure 7: (color online) Some molecular orbitals (iso plots) of icosahedral B_{12}, obtained from the first principles DFT/B3LYP calculations.

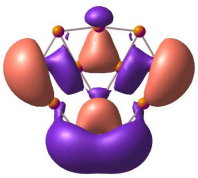

(a) HOMO-1

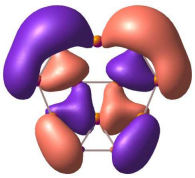

(b) HOMO

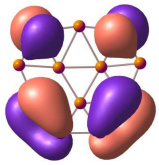

(c) LUMO

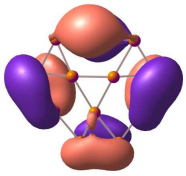

(d) LUMO+1

Figure 8: (color online) Some molecular orbitals (iso plots) of quasi-planar B_{12}, obtained from the first principles DFT/B3LYP calculations.

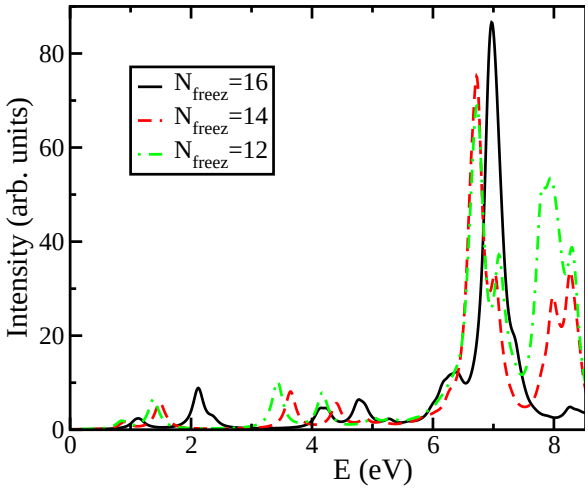

Figure 9: (color online) Convergence of the linear absorption spectrum of icosahedral B_{12} computed using the INDO-MRSDCI method for decreasing number of frozen occupied orbitals. A line width of 0.1 eV was used to compute the spectra.

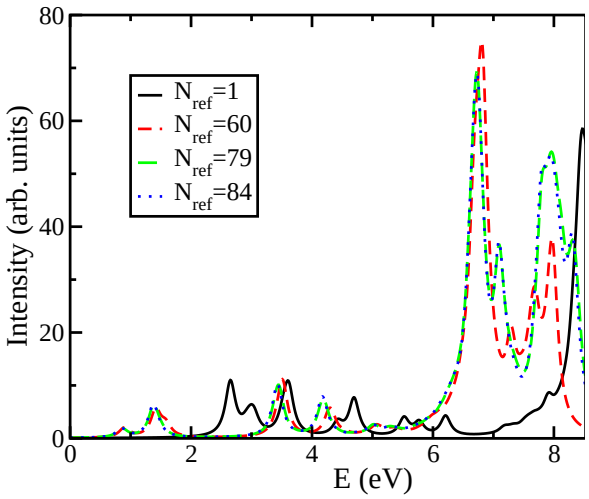

Figure 10: (color online) Convergence of the linear absorption spectrum of icosahedral B_{12} with increasing number of reference configurations (N_{ref}) in the MRSDCI wave function with $N_{freez} = 12$. A line width of 0.1 eV was used to compute the spectra.

Table IV: Excitation energies, E, and many-particle wave functions of the excited states corresponding to some of the peaks in the INDO-MRSDCI linear absorption spectrum of icosahedral B_{12} (*cf.* Fig. 4a), along with the squares of their dipole coupling ($\mu^2 = \sum_i |\langle f|d_i|G\rangle|^2$) to the ground state. $|f\rangle$ denotes the excited state in question, $|G\rangle$, the ground state, and d_i is the i-th Cartesian component of the electric dipole operator. In the wave function, the bracketed numbers are the CI coefficients of a given electronic configuration. Symbols H/L denote HOMO/LUMO orbitals.

Peak	E (eV)	μ^2(a.u.)	Wave Function
IV	4.1563	0.0919	$\|H \to L+3\rangle(0.4902)$
			$\|H \to L; H \to L+6\rangle(0.4622)$
			$\|H \to L; H \to L+5\rangle(0.4070)$
V	5.0252	0.0171	$\|H-3 \to L; H \to L+2\rangle(0.3519)$
			$\|H-2 \to L; H \to L+2\rangle(0.3322)$
VII	7.0917	0.3664	$\|H \to L+10\rangle(0.5795)$
			$\|H \to L; H \to L+9\rangle(0.4872)$
			$\|H \to L+1; H \to L+9\rangle(0.3962)$
IX	8.2770	0.1232	$\|H-2 \to L; H \to L+5\rangle(0.3093)$
			$\|H-2 \to L; H \to L+3\rangle(0.2999)$
	8.3141	0.0905	$\|H \to L+1; H-1 \to L+2\rangle(0.3300)$
			$\|H-1 \to L+1; H \to L+4\rangle(0.2080)$
			$\|H-1 \to L+3\rangle(0.2043)$
	8.3178	0.0974	$\|H-2 \to L+1; H \to L+2\rangle(0.2716)$
			$\|H \to L+4; H-1 \to L\rangle(0.2525)$
			$\|H-1 \to L+1; H \to L+65\rangle(0.2346)$
			$\|H-2 \to L; H \to L+4\rangle(0.2121)$

Table V: This table contains information pertinent to some of the peaks of the INDO-MRSDCI optical absorption spectrum of the quasi-planar B_{12}, as shown in Fig. 5a. The symbols have the same meaning as in the caption of table IV.

Peak	E(eV)	μ^2(a.u.)	Wave function
V	10.7578	0.0279	$\|H \rightarrow L+8\rangle(0.6230)$
			$\|H-5 \rightarrow L+2\rangle(0.4956)$
			$\|H \rightarrow L+1; H \rightarrow L+1\rangle(0.2400)$
			$\|H-5 \rightarrow L\rangle(0.1807)$
VI	11.2054	0.2187	$\|H-1 \rightarrow L+9\rangle(0.4144)$
			$\|H-5 \rightarrow L\rangle(0.3539)$
			$\|H \rightarrow L+10\rangle(0.3255)$
			$\|H-5 \rightarrow L+2\rangle(0.3049)$
			$\|H \rightarrow L+8\rangle(0.2973)$
			$\|H \rightarrow L; H \rightarrow L\rangle(0.1953)$
VII	12.3562	0.1598	$\|H \rightarrow L+10\rangle(0.6469)$
			$\|H-3 \rightarrow L+3\rangle(0.3408)$
			$\|H \rightarrow L+12\rangle(0.2985)$
			$\|H \rightarrow L+13\rangle(0.2299)$
			$\|H \rightarrow L+8\rangle(0.2095)$
			$\|H-1 \rightarrow L+11\rangle(0.2063)$
			$\|H-4 \rightarrow L+5\rangle(0.1792)$
VIII	13.1344	0.0300	$\|H-3 \rightarrow L+3\rangle(0.6665)$
			$\|H-4 \rightarrow L+5\rangle(0.3184)$
			$\|H \rightarrow L+13\rangle(0.2582)$
			$\|H-2 \rightarrow L+2\rangle(0.2586)$
			$\|H-1 \rightarrow L; H \rightarrow L+3\rangle(0.2186)$
			$\|H-4 \rightarrow L+7\rangle(0.1921)$
			$\|H-4 \rightarrow L; H \rightarrow L+2\rangle(0.1574)$